

*Antonio Campanile, Department of Naval Engineering, University “Federico II”, Naples
Masino Mandarino, Department of Naval Engineering, University “Federico II”, Naples
Vincenzo Piscopo, Department of Naval Engineering, University “Federico II”, Naples*

DESIGN CHARTS FOR CLAMPED ORTHOTROPIC PLATES

Summary

This paper focuses on the application of orthotropic plate bending theory, particularly of Schade’s design curves, to the scantlings assessment of deck primary supporting members in absence of pillars. Preliminarily, a review of Schade’s works is presented, paying attention to the design curves relative to the plate with all edges clamped, that are almost totally incomplete. Therefore a numerical solution for the clamped orthotropic plate equation is obtained. The Ritz method is adopted, expressing the vertical displacement field by a double cosine trigonometric series, whose coefficients are determined by solving a linear equation system. Several design curves are proposed for different values of the torsional parameter η_t in a range comprised between 0 and 1, as functions of the virtual aspect ratio ρ comprised between 1 and 8, in order to estimate the asymptotic behaviour of the orthotropic plate when $\rho \rightarrow \infty$. Finally, a numerical application relative to the deck of a fast ferry is presented.

Key words: orthotropic plate bending; Ritz method; stiffened plate.

1. Introduction

Schade, 1942, proposed some practical general design curves, based on the “orthotropic plate” theory, in order to obtain a rapid, but accurate, dimensioning of plating stiffeners. Schade considered four types of boundary conditions for the orthotropic partial differential equation: all edges rigidly supported but not fixed; both short edges clamped, both long edges supported; both long edges clamped, both short edges supported; all edges clamped. The last case with all edges clamped was left almost totally incomplete. The few data useful for this boundary condition were taken from Timoshenko et al., 1959, and Young, 1940, as given for the isotropic plate only for the torsional coefficient value $\eta_t = 1$ and for a range of the virtual aspect ratio ρ comprised between 1 and 2.

In this work a numerical solution of the clamped orthotropic plate equation is obtained. Numerical results are presented in a series of charts similar to those ones given by Schade.

2. A numerical solution of the clamped rectangular orthotropic plate equation

Orthotropic plate theory refers to materials which have different elastic properties along two orthogonal directions. In order to apply this theory to panels having a finite number of stiffeners, it is necessary to idealize the structure, assuming that the structural properties of the stiffeners may be approximated by their average values, which are assumed to be distributed uniformly over the width and the length of the plate.

The deflection field in bending is governed by the so called Huber’s differential equation:

$$D_x \frac{\partial^4 w}{\partial x^4} + 2H \frac{\partial^4 w}{\partial x^2 \partial y^2} + D_y \frac{\partial^4 w}{\partial y^4} = p(x, y) \quad (1)$$

where:

- D_x is the unit flexural rigidity around the y axis;
- D_y is the unit flexural rigidity around the x axis;
- $H = D_{xy} + 2D_{33} = \eta_t \sqrt{D_x D_y}$ according to the definition by Schade;
- p is the pressure load over the surface.

It is noticed that the behaviour of the isotropic plate with the same flexural rigidities in all directions is a special case of the orthotropic plate problem.

Indicating with n the normal external to the plate contour, a numerical solution of the orthotropic plate equation with the boundary conditions:

$$w = 0 \quad \text{and} \quad \frac{\partial w}{\partial n} = 0 \quad (2)$$

along all edges is presented. Two solution methods are available: the double cosine series and the Hencky’s method. The second one is well known to converge quickly but does pose some difficulties with regard to programming due to over/underflow problems in the evaluation of hyperbolic trigonometric functions with large arguments. The double cosine series method, instead, is devoid of the over/underflow issue but is known to converge very slowly.

If a and b are the plate lengths in the x and y directions respectively, the vertical displacement field may be expressed by means of the following double cosine series whose terms satisfy the boundary conditions (2):

$$w(\xi, \eta) = \sum_{m=1}^M \sum_{n=1}^N (1 - \cos 2\pi m \xi) \cdot (1 - \cos 2\pi n \eta) w_{m,n} \quad (3)$$

where:

$$x = a\xi \quad \text{with} \quad 0 \leq \xi \leq 1 \quad ; \quad y = b\eta \quad \text{with} \quad 0 \leq \eta \leq 1 \quad (4)$$

The unknown coefficients $w_{m,n}$ may be determined using the Ritz method, searching for the minimum of the total energy, which is given by:

$$V = \frac{1}{2} \int_A \left[D_x \left(\frac{\partial^2 w}{\partial x^2} \right)^2 + 2D_{xy} \frac{\partial^2 w}{\partial x^2} \frac{\partial^2 w}{\partial y^2} + 4D_{33} \left(\frac{\partial^2 w}{\partial x \partial y} \right)^2 + D_y \left(\frac{\partial^2 w}{\partial y^2} \right)^2 \right] - \int_A w p dA \quad (5)$$

Applying the generalized integration by parts formula, equation (5) reduces in this case to:

$$V = \frac{1}{2} \int_A \left[D_x \left(\frac{\partial^2 w}{\partial x^2} \right)^2 + 2H \frac{\partial^2 w}{\partial x^2} \frac{\partial^2 w}{\partial y^2} + D_y \left(\frac{\partial^2 w}{\partial y^2} \right)^2 \right] - \int_A w p dA \quad (6)$$

which can be re-written in the form:

$$\Pi = \frac{V}{ab} = \frac{1}{2} \int_0^1 \int_0^1 \left[\frac{D_x}{a^4} \left(\frac{\partial^2 w}{\partial \xi^2} \right)^2 + \frac{2H}{a^2 b^2} \frac{\partial^2 w}{\partial \xi^2} \frac{\partial^2 w}{\partial \eta^2} + \frac{D_y}{b^4} \left(\frac{\partial^2 w}{\partial \eta^2} \right)^2 \right] d\xi d\eta - \int_0^1 \int_0^1 w p d\xi d\eta \quad (7)$$

The stationary point is obtained imposing the following $M \times N$ equations system:

$$\frac{\partial \Pi}{\partial w_{m,n}} = 0 \quad \text{for} \quad m = 1, \dots, M; \quad n = 1, \dots, N \quad (8)$$

So, considering p as uniformly distributed, the generic equation, for $m = \bar{m}$ and $n = \bar{n}$, assumes the form:

$$\frac{\partial}{\partial w_{\bar{m}, \bar{n}}} \int_0^1 \int_0^1 \left[\frac{D_x}{a^4} \left(\frac{\partial^2 w}{\partial \xi^2} \right)^2 + \frac{2H}{a^2 b^2} \frac{\partial^2 w}{\partial \xi^2} \frac{\partial^2 w}{\partial \eta^2} + \frac{D_y}{b^4} \left(\frac{\partial^2 w}{\partial \eta^2} \right)^2 \right] d\xi d\eta = 2p \frac{\partial}{\partial w_{\bar{m}, \bar{n}}} \int_0^1 \int_0^1 w d\xi d\eta \quad (9)$$

Defining the non dimensional vertical displacements:

$$\delta = \frac{w}{pb^4/D_y} \quad ; \quad \delta_{m,n} = \frac{w_{m,n}}{pb^4/D_y} \quad (10)$$

from the equations (3) and (9) it is obtained:

$$4\pi^4 \left\{ \frac{1}{\rho^4} \left[m^{-4} \delta_{m,n} + \sum_{n=1}^N 2m^{-4} \delta_{m,n} \right] + n^{-4} \delta_{m,n} + \sum_{m=1}^M 2n^{-4} \delta_{m,n} + \frac{2\eta_t}{\rho^2} m^{-2} n^{-2} \delta_{m,n} \right\} = 1 \quad (11)$$

where ρ is the virtual side ratio.

Even if the double cosine trigonometric series converges very slowly, adopting sufficiently high values for M and N , it is possible to obtain a very accurate solution of the equation (1) with the boundary conditions (2).

3. Characterization of the behaviour of clamped stiffened plates

The orthotropic plate bending theory can be applied to a plate reinforced by two systems of parallel beams spaced equal distances apart in the x and y directions. The rigidities D_X and D_Y of equation (1) can be specialized as follows:

$$D_X = \frac{EI_{eX}}{s_X} = Ei_X \quad D_Y = \frac{EI_{eY}}{s_Y} = Ei_Y \quad (12)$$

where E is the Young's modulus, s_X (s_Y) is the distance between girders (transverses), I_{eX} (I_{eY}) is the moment of inertia, including effective width b_{eX} (b_{eY}) of plating, of long (short) repeating stiffeners.

The torsional coefficient η_t and the virtual side ratio ρ can be specialized according to Schade's works:

$$\eta_t = \sqrt{\frac{i_{pX}i_{pY}}{i_Xi_Y}} \quad \rho = \frac{a}{b} \sqrt{\frac{i_Y}{i_X}} \quad (13)$$

where i_{pX} (i_{pY}) is the moment of inertia of effective breadth of plating working with long (short) supporting stiffeners per unit length. In the following r_{Xp} (r_{Yp}) is the vertical distance of the associated plating working with long (short) supporting stiffeners from the section neutral axis, while r_{Xf} (r_{Yf}) is the distance of the free flange from the section neutral axis.

The meaning of the two parameters is quite clear. In particular, the torsional coefficient η_t , which lies between 0 and 1, exists because only the plating is subject to horizontal shear, while both the plating and stiffeners are subject to bending stress. Obviously $\eta_t = 1$, and $i_{pX} = i_{pY} = i_X = i_Y$, represents the isotropic plate case. The virtual side ratio ρ is the plate side ratio modified in accordance with the unit stiffnesses in the two directions; as usual, it has been admitted that ρ is always equal to or greater than unity. In the next the quantities represented in the diagrams are presented.

Deflection at center, fig.1: the vertical displacement at the plate center ($\eta=\xi=0.5$) is the maximum and is so expressed:

$$w_{\max} = k_W \frac{pb^4}{Ei_Y} \quad \text{where:} \quad k_W(\rho, \eta) = \sum_{m=1}^M \sum_{n=1}^N \delta_{m,n} (1 - \cos \pi m)(1 - \cos \pi n) \quad (14)$$

Edge bending stress in plating, fig.2: these curves give the bending stress in the plating at the centers of edges where fixity exists. The stress at the center of such an edge may be treated as the maximum along that edge. The maximum stresses in the plating in the long and short directions respectively are:

$$\sigma_{XpSUP} = k_{XpSUP}(\rho, \eta) \frac{pb^2 r_{Xp}}{\sqrt{i_X i_Y}} \quad \sigma_{YpSUP} = k_{YpSUP}(\rho, \eta) \frac{pb^2 r_{Yp}}{i_Y} \quad (15)$$

where:

$$k_{XpSUP}(\rho, \eta) = \frac{1}{\rho^2} \frac{4\pi^2}{1-\nu^2} \sum_{m=1}^M \sum_{n=1}^N \delta_{m,n} m^2 (1 - \cos \pi m) \quad (16.1)$$

$$k_{YpSUP}(\rho, \eta) = \frac{4\pi^2}{1-\nu^2} \sum_{m=1}^M \sum_{n=1}^N \delta_{m,n} n^2 (1 - \cos \pi n) \quad (16.2)$$

Edge bending stress in free flanges, fig.3: these curves give the bending stress in the free flanges at the centers of edges where fixity exists. The stress at the center of such an edge may be treated as the maximum along that edge. The maximum stresses in the free flanges for girders and transverses are respectively:

$$\sigma_{xfsUP} = -k_{xfsUP}(\rho, \eta) \frac{pb^2 r_{xf}}{\sqrt{i_x i_y}} \quad \sigma_{yfsUP} = -k_{yfsUP}(\rho, \eta) \frac{pb^2 r_{yf}}{i_y} \quad (17)$$

where:

$$k_{xfsUP}(\rho, \eta) = \frac{4\pi^2}{\rho^2} \sum_{m=1}^M \sum_{n=1}^N \delta_{m,n} m^2 (1 - \cos \pi m) \quad (18.1)$$

$$k_{yfsUP}(\rho, \eta) = 4\pi^2 \sum_{m=1}^M \sum_{n=1}^N \delta_{m,n} n^2 (1 - \cos \pi n) \quad (18.2)$$

It is important to note that when $\rho \rightarrow \infty$ k_{yfsUP} is substantially independent on η_t and is equal to $1/12$, that is the beam theory value. Furthermore the curves show that for low values of η_t the maximum deflections and stresses parallel to the short direction occur at values of ρ between 1.5 and 2.0: this indicates that the long beams add to the load taken by the short beams, instead of helping to support it.

In order to verify the goodness of the method, the following tables shows a comparison between the values obtained applying the Ritz method and the ones taken from Timoshenko et al., 1959, for the isotropic plate.

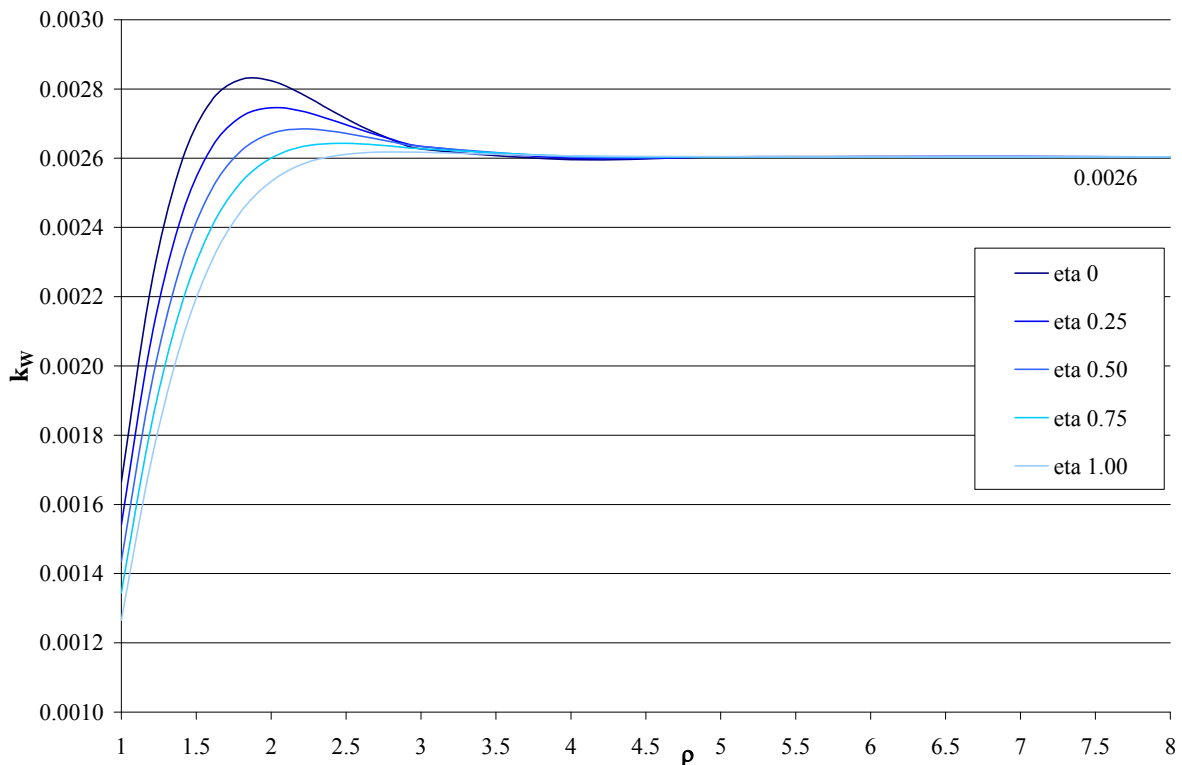


Fig. 1 Deflection at center

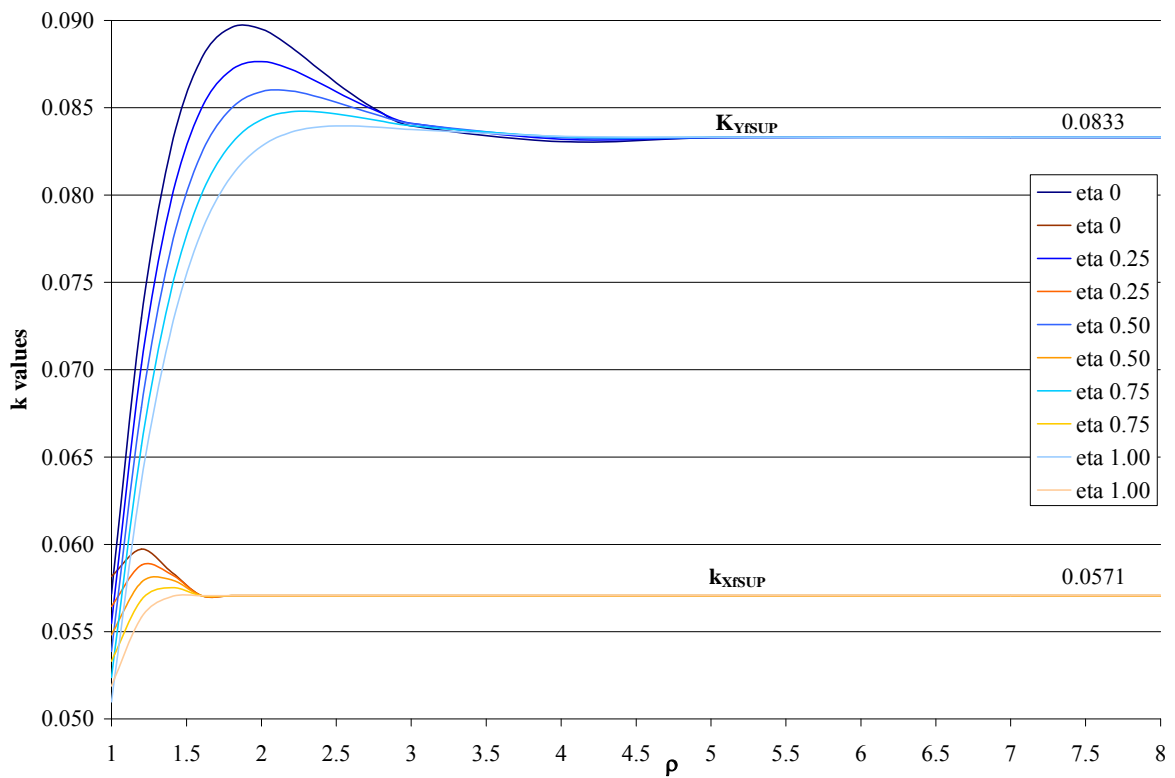
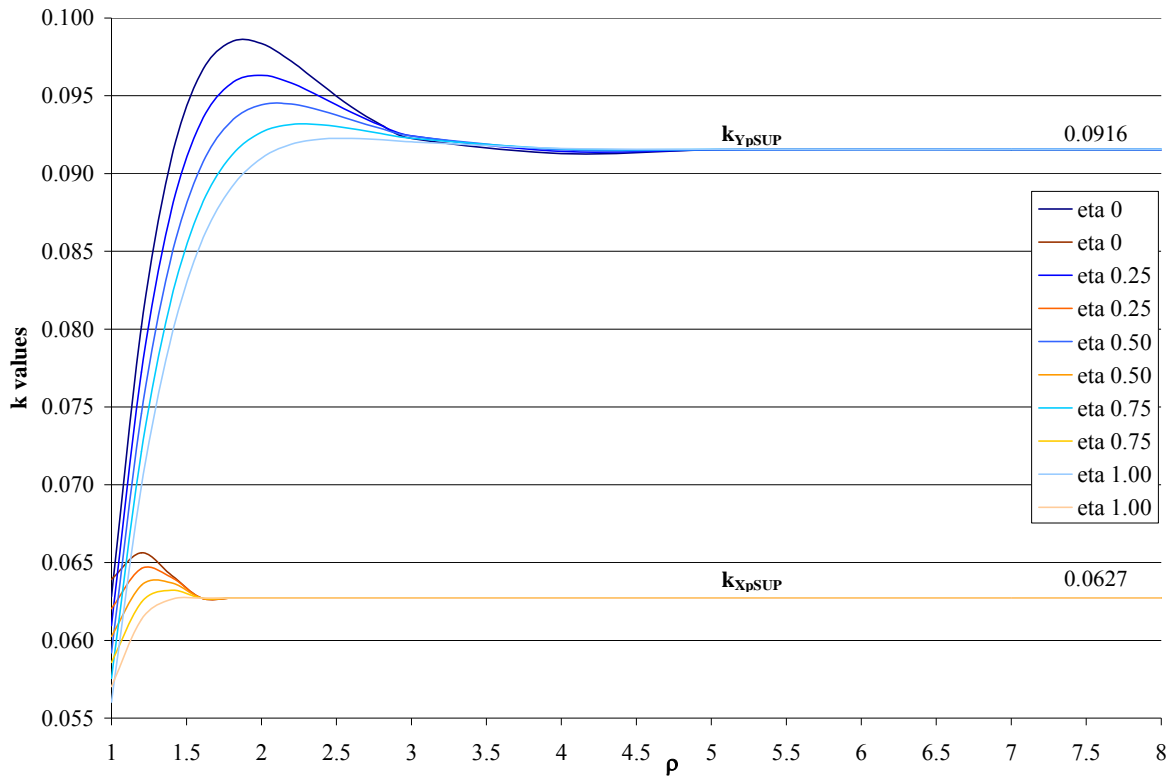


Table 1 Comparison between Timoshenko and actual data

ρ	Deflection at center		Edge bending moment in short direction		Edge bending moment in long direction	
	Timoshenko	k_W $\eta_t = 1.00$	Timoshenko	$(1-\nu^2) K_{YpSUP}$ $\eta_t = 1.00$	Timoshenko	$(1-\nu^2) K_{XpSUP}$ $\eta_t = 1.00$
1.00	0.00126	0.00126	0.0513	0.0510	0.0513	0.0510
1.20	0.00172	0.00172	0.0639	0.0636	0.0554	0.0558
1.40	0.00207	0.00207	0.0726	0.0724	0.0568	0.0570
1.60	0.00230	0.00230	0.0780	0.0779	0.0571	0.0571
1.80	0.00245	0.00245	0.0812	0.0811	0.0571	0.0571
2,00	0.00254	0.00253	0.0829	0.0828	0.0571	0.0571
∞	0.00260	0.00260	0.0833	0.0833	0.0571	0.0571

4. Convergence of the method

In the following, the influence of the number of harmonics on k values is shown. Particularly, assuming $\rho = 5$ and $\eta = 0.50$, $M=N$ has been varied from 5 up to 100, in order to obtain a number of harmonics comprised between 25 and 10000. If the number of harmonics is > 4900 , i.e. $M=N > 70$, a good convergence in the assessment of k values, and then of the proposed curves, is obtained for practical purposes, as it can be appreciated from fig. 4, 5, 6.

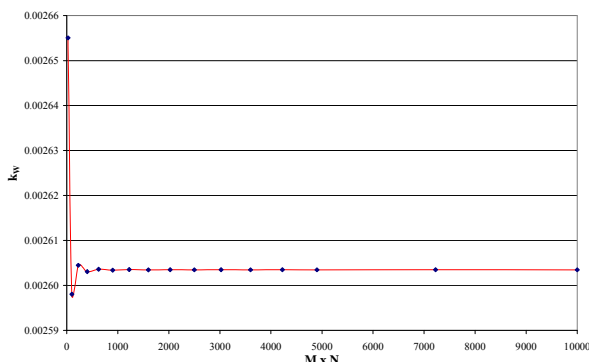


Fig. 4 K_W convergence

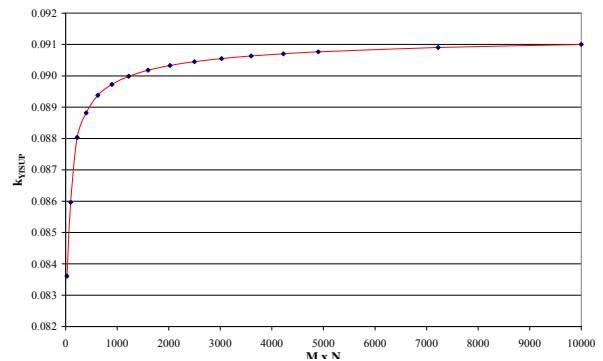


Fig. 5 Design charts for clamped orthotropic plates

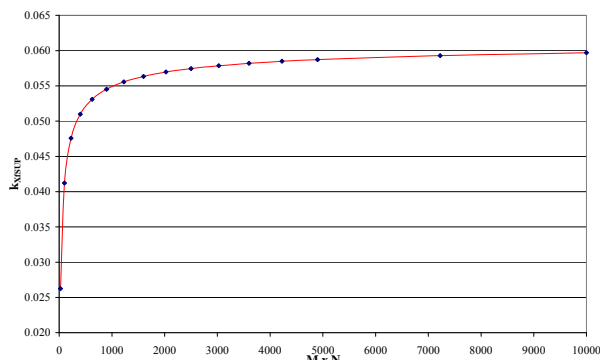


Fig. 6 K_{XpSUP} convergence

5. Application to a ro-ro fast ferry deck

The orthotropic plate bending theory has been applied to the garage deck of a fast ferry, with a displacement of 1420 t, considered in [6]. The deck spans 80 m in length and 16 m in breadth; its thickness is 8 mm. Both transverse beams and longitudinal girders are T sections 320x150x10x15 mm, 2 m spaced. The material is high-strength steel with $R_{eH} = 355 \text{ N/mm}^2$.

The maximum equivalent pressure load $p_{eq,max}$ acting on transverse beams has been estimated as 4914 N/m^2 , according to RINA rules, 2005. To this extent, it has been assumed a typical vehicle axle load of 1.2 t, 7 vehicles located on the transverse beam and a vertical acceleration of 0.909 g.

To enter relevant charts, the plate parameters have been assessed: $\rho = 5$; $\eta_t = 0.19$. Because of the large value of the virtual side ratio, as usual for garage decks, the asymptotic values hold, that is:

$$k_{YFSUP} = 0.0833 \qquad k_{XFSUP} = 0.0571$$

Hence, maximum stresses in transverses and girders are derived:

$$\sigma_{YFSUP} = 205 \text{ N/mm}^2 \qquad \sigma_{XFSUP} = 141 \text{ N/mm}^2$$

For comparison, a coarse mesh FE analysis has been performed, obtaining stresses close to the previous ones, i.e. $\sigma_{YFSUP} = 214 \text{ N/mm}^2$; $\sigma_{XFSUP} = 146 \text{ N/mm}^2$

Obtained results are relative to a uniform pressure acting on the deck. In this respect, it must be pointed out that $p_{eq,max}$ corresponds to the vehicle axle located directly on a transverse beam and this coincidence cannot obviously occur at every transverse beam. In other terms, the actual load is not evenly distributed, at least longitudinally; $p_{eq,max}$ has to be considered as a peak value and corresponding stress values as upper bound values.

For instance, on the basis of longitudinal dimensions of the typical vehicle, the actual equivalent pressure distribution can be characterized by:

$$p_{eq,mean} = 0.75 p_{eq,max} ; \quad COV = 0.26$$

Then, a lower bound of acting stresses can be evaluated considering a uniform pressure $p_{eq,mean}$; correspondingly it is obtained:

$$\sigma_{YFSUP} = 161 \text{ N/mm}^2 \qquad \sigma_{XFSUP} = 105 \text{ N/mm}^2$$

The significance of these values has been stressed by an independent analysis where the actual pressure distribution has been taken into account; the following values have been obtained:

$$\sigma_{YFSUP} = 164 \text{ N/mm}^2 \qquad \sigma_{XFSUP} = 100 \text{ N/mm}^2$$

These values are very close to the previous ones relative to $p = p_{eq,mean} = \text{const}$; it must be concluded that there is a significant stress re-distribution due to the longitudinal rigidities. Moreover, obtained results suggest the possibility of evaluating acting stresses with reference to the mean equivalent pressure load evenly distributed over the deck. Obviously, this simplified approach, and its range of applicability, should be verified extending the analysis to typical deck configurations and appropriate load distributions.

6. Conclusions

In this work the orthotropic rectangular plate bending equation with all edges clamped has been solved adopting the Ritz method. Numerical calculations have been systematically performed varying two non-dimensional parameters, namely the virtual side ratio and the torsional coefficient. Response non-dimensional parameters, in terms of maximum deflection and maximum stresses, are given in a series of charts for their easy application. Some comparisons with well known published data and FEM analyses give a validation to the method. The method has been applied to the garage deck of a fast ferry, taking into account, according to the geometrical and mass characteristics of the reference vehicle, two different pressure loads, representative of the upper and lower bounds.

REFERENCES

- [1] Schade H.A., 'Design Curves for Cross-Stiffened Plating under Uniform Bending Load', *Trans. SNAME*, 49, 1941.
- [2] Timoshenko S., Woinowsky-Krieger S., 'Theory of Plates and Shells', Mc-Graw-Hill Book Company, 1959.
- [3] Young D., 'Analysis of Clamped Rectangular Plates', *Journal of Applied Mechanics*, Volume 7, No.4, December 1940.
- [4] Fiorenza R., 'Appunti delle lezioni di Analisi Funzionale', Gli Strumenti di Coinor, 2005.
- [5] RINA, 'Rules for the Classification of Ships', 2005.
- [6] Campanile A., Mandarino M., Piscopo V., 'Considerations on dimensioning of garage decks', ICMRT 2007.